Global J. Environ. Sci. Manage. 13(1): 231-250, Winter 2027, Serial #49

Global Journal of Environmental Science and Management
(GJESM)

Homepage: https://www.gjesm.net/

Podcasts

ORIGINAL RESEARCH ARTICLE

Ecological diversity in soil properties and bacterial communities in tropical coastal areas with contrasting electrical conductivity

L. Fauziah[1,2], Y. Nuraini[3], Soemarno[3], N.D. Lestari[3], Djajadi[2], N. Aini[4,]*

[1]*Postgraduate Program, Faculty of Agriculture, Brawijaya University, Jl., Malang, 65145 Indonesia*

[2]*Research Center for Estate Crops, Research Organization for Agriculture and Food, the National Research and Innovation Agency of the Republic of Indonesia, Jl., Cibinong, Bogor, 16911 Indonesia*

[3]*Department of Soil Science, Faculty of Agriculture, Brawijaya University, Jl., Malang, 65145 Indonesia*

[4]*Department of Agronomy, Faculty of Agriculture, Brawijaya University, Jl., Malang, 65145 Indonesia*

ARTICLE INFO

Article History:
Received 12 May 2026
Revised 17 July 2026
Accepted 19 August 2026

Keywords:
Coastal soil
Electrical conductivity
Saline soil
Soil bacterial community
Soil physicochemical properties
Tropical agricultural soil

DOI:10. 22034.gjesm.2027.01.11

ABSTRACT

BACKGROUND AND OBJECTIVES: Coastal soil salinization is an environmental constraint that alters soil physicochemical conditions and may restructure microbial communities, while field patterns may also reflect land use and co-varying soil properties. The study objectives were to characterize soil physicochemical conditions together with bacterial diversity, composition, community dissimilarity, and predicted ecological functions at three tropical coastal sites in Palang, Tuban, East Java, with contrasting electrical conductivity.

METHODS: Electrical conductivity at sampling sites PA8, PA9, and PA10 was 13.68, 3.74, and 0.50 decisiemens per meter, respectively. A single composite soil sample was collected and analyzed from each site and subjected to near full-length bacterial small-subunit ribosomal ribonucleic acid gene amplicon sequencing. Following quality filtering and denoising, amplicon sequence variants were resolved, and taxonomic assignments were performed against a curated ribosomal reference database. Observed richness, Shannon and Gini-Simpson indices, Bray-Curtis and Weighted UniFrac principal coordinate analyses, taxonomic relative abundance, and taxonomy-based predicted functions were summarized descriptively. Site-to-site variations in exchangeable sodium, organic carbon, cation exchange capacity, phosphorus availability, soil texture, and culturable bacterial abundance were also compared among sites**.** Due to the confounding of site identity, electrical conductivity, land use, and other edaphic properties, replicated inference of salinity effects was not feasible.

FINDINGS: PA8 had 2,052 observed sequence variants and a Shannon index of 9.61; PA9 had 5,205 variants and a Shannon index of 11.39; and PA10 had 3,145 variants and a Shannon index of 11.03. Taxonomic profiles differed among sites. PA8 was characterized by Bacillota, Bacillales, and Incertae_Sedis_14; PA9 by Bacillota/Pseudomonadota, Bacillales, and Neobacillus; and PA10 by Chloroflexota, Anaerolineales, and UTCFX1. Weighted UniFrac distances were 0.3266 for PA9–PA10, 0.4850 for PA8–PA9, and 0.5226 for PA8–PA10. Predicted chemoheterotrophy accounted for 20.46 percent, 16.97 percent, and 23.88 percent of post-filter reads at sites PA8, PA9, and PA10, respectively. PA8 also had the highest exchangeable sodium, whereas PA10 had the highest organic carbon, cation exchange capacity, Olsen-available phosphorus, and culturable bacterial abundance**.**

CONCLUSION: While intra-site analyses revealed marked heterogeneity in physicochemical parameters and bacterial community structures, the observational framework of this study limits direct causal attribution to salinity gradients and restricts the extrapolation of findings to wider salinity categories. The findings provide a site-specific environmental baseline and hypotheses for future replicated studies.

This is an open access article under the CC BY license (http://creativecommons.org/licenses/by/4.0/)

NUMBER OF REFERENCES	NUMBER OF FIGURES	NUMBER OF TABLES
51	5	5

*Corresponding Author:
Email: nra-fp@ub.ac.id
Phone: +62813 3411 0303
ORCID: 0000-0002-7480-8243

Note: Discussion period for this manuscript open until March 01, 2027 on GJESM website at the “Show Article”.

INTRODUCTION

Coastal soil salinization is a major environmental constraint in tropical agricultural landscapes because excessive soluble salts can reduce soil water availability, disturb ionic and nutrient balance, and impose osmotic and ionic stress on plants and soil microorganisms (Dong *et al.*, 2022; Hailu and Mehari, 2021; Tarolli *et al.*, 2024). In coastal environments, these hydrological stresses are frequently exacerbated by seawater intrusion, saline water influxes, impeded drainage, and evaporative enrichment. For soil bacteria, increased osmotic stress and ionic imbalance can constrain growth and resource use, modify competitive interactions, and favor taxa able to maintain cellular homeostasis under saline conditions. Consequently, bacterial richness, evenness, taxonomic composition, and phylogenetically structured community dissimilarity can exhibit substantial spatial variation across salt-affected soils. Furthermore, these spatial distributions can be modulated by confounding covariates, including organic carbon concentrations, soil potential of hydrogen (pH), moisture dynamics, sodium chemistry, and anthropogenic land use (Dong *et al.*, 2022; Li *et al.*, 2023; Rath *et al.*, 2019). Such interactions between agroecological conditions, soil chemical properties, and microbial diversity have also been documented in tropical agricultural systems, highlighting the importance of evaluating microbial patterns alongside site-specific environmental characteristics (Tarigan *et al.*, 2026). Electrical conductivity (EC) is therefore used here as the descriptor of soluble-salt conditions, whereas sodicity-related measurements are treated separately. 16S ribosomal ribonucleic acid (16S rRNA) gene amplicon sequencing enables culture-independent characterization of bacterial communities and is widely used to compare community composition across environmental samples (Dreier *et al.*, 2022). Empirical evaluations of agricultural and coastal saline soils consistently demonstrate distinct shifts in bacterial richness, structural diversity, and taxonomic configurations under varying salinity regimes. The magnitude and direction of these patterns are strongly context dependent and may covary with pH, organic carbon, moisture, sodium-related chemistry, and other site properties (Dong *et al.*, 2022; Hindersah *et al.*, 2023; Li *et al.*, 2023; Mucsi *et al.*, 2024; Rath *et al.*, 2019). Mechanistically, elevated soluble salts can impose osmotic constraints and alter nutrient and cation availability, whereas pH, organic carbon, and moisture modify substrate supply and habitat conditions. Consequently, such interconnected edaphic drivers modulate microbial assembly by governing taxon persistence and relative abundance profiles, which directly shape both within-sample richness and between-sample structural divergence. Thus, current evidence supports salinity as an important ecological filter but does not imply a universal or strictly monotonic bacterial response across soils. The contribution of salinity cannot be separated from co-varying soil properties without independent biological replication or a design that decouples those factors. Such constraints are particularly salient within tropical coastal agroecosystems, where salinity regimes evolve amidst complexly varied agricultural practices and edaphic management frameworks. The broader importance of integrating biodiversity considerations with coastal landscape management has likewise been emphasized in studies of mangrove-based coastal resilience and ecosystem rehabilitation (Utomo *et al.*, 2026; Yuliana *et al.*, 2026). Taxonomy-based tools such as functional annotation of prokaryotic taxa (FAPROTAX) can additionally generate hypotheses about potential ecological functions, but these predictions do not measure functional genes, transcripts, enzymes, or process rates (Louca *et al.*, 2016; Sansupa *et al.*, 2021). Accordingly, the knowledge gap addressed here is not whether salinity affects soil bacteria in general. Instead, it concerns the limited site-specific baseline information for tropical coastal agricultural soils of East Java. To address this gap, this study integrates nearly full-length 16S rRNA profiling with empirical soil chemistry, amplicon sequence variant (ASV) diversity, taxonomic composition, pairwise community dissimilarity, and conservatively

interpreted functional potential. The present study therefore provides a descriptive survey of three geographically distinct coastal sites in Palang, Tuban, with contrasting measured EC. PA8, PA9, and PA10 were each represented by one composite sequencing sample. Consequently, site identity, land use, EC, and other soil properties were confounded, and the study was not designed to estimate replicated salinity-treatment effects or isolate salinity from other site characteristics. Specifically, the objectives of this study are to document soil environmental parameters and to describe observed ASV richness and diversity, bacterial taxonomic relative abundance, pairwise community dissimilarity, and inferred ecological functions across three coastal gradients characterized by divergent EC levels. Site-specific environmental and bacterial patterns were identified to guide future replicated studies. The present study was conducted in coastal agricultural soils of Palang, Tuban, East Java, Indonesia in 2025.

MATERIALS AND METHODS

Research approach and design

This study was an exploratory, field-based observational survey of three geographically distinct sites within Palang Subdistrict that were purposively selected to span contrasting measured EC conditions. In order to mitigate potential temporal confounding, sampling across all three locations was conducted within the same synchronized field campaign in November 2025. The sampling sites, coded PA8, PA9, and PA10, were individual sites rather than biological replicates of salinity or EC treatments, and one composite sequencing sample was analyzed from each site. Site selection did not ensure that bacterial differences represented EC alone. Consequently, potential confounding persisted among site-specific factors, including land-use patterns, sodium chemistry, organic carbon dynamics, cationic profiles, management regimens, and both quantified and unquantified environmental parameters. Accordingly, alpha-diversity metrics, taxonomic profiles, ordination patterns, and predicted functions were interpreted descriptively, and no inferential test was used to claim a salinity-treatment effect.

Study area

This study was conducted at three coastal sites in Palang Subdistrict, Tuban Regency, East Java, Indonesia (Fig. 1). PA8 was located in Leran Wetan, Palang, Tuban, at 6°54′26.4″ south (S) 112°10′12.6″ east (E). PA9 was located in Karang Lor, Cepokrejo, Palang, Tuban, at 6°54′47.2″ south and 112°09′51.6″ east. PA10 was located in Wangun Bara, Wangun, Palang, Tuban, at 6°56′09.1″ south and 112°09′52.8″ east. Field records identified the land-use categories as a salt-producing pond at PA8, paddy/fallow land at PA9, and paddy land at PA10. These land-use disparities represent potential site-level confounding variables rather than experimentally controlled experimental parameters. Site selection was based on contrasting measured EC rather than replicated salinity treatments. EC was determined using a 1:5 soil-to-water suspension and interpreted using the criteria of Eviati *et al.* (2023), in which <1; 1–2; 2–3; 3–4; and >4 dS/m correspond to very low, low, moderate, high, and very high EC classes, respectively. On this basis, PA8 (13.68 dS/m), PA9 (3.74 dS/m), and PA10 (0.50 dS/m) corresponded to very high, high, and very low EC classes. To avoid implying true experimental replication, the study locations are designated throughout the comparative interpretation as the highest-EC site (PA8), intermediate-EC site (PA9), and lowest-EC site (PA10). These descriptors are site specific and do not constitute formal saline, sodic, or saline-sodic soil classification.

Soil sample collection

At each site, soil was collected from five sampling points without a fixed geometric sampling pattern, with approximately 10 meters (m) spacing between successive points. Surface litter and vegetation were removed before sampling. Approximately 500 grams (g) of soil was retrieved from the entire 0–20 centimeters (cm) depth layer at each designated point using a clean shovel,

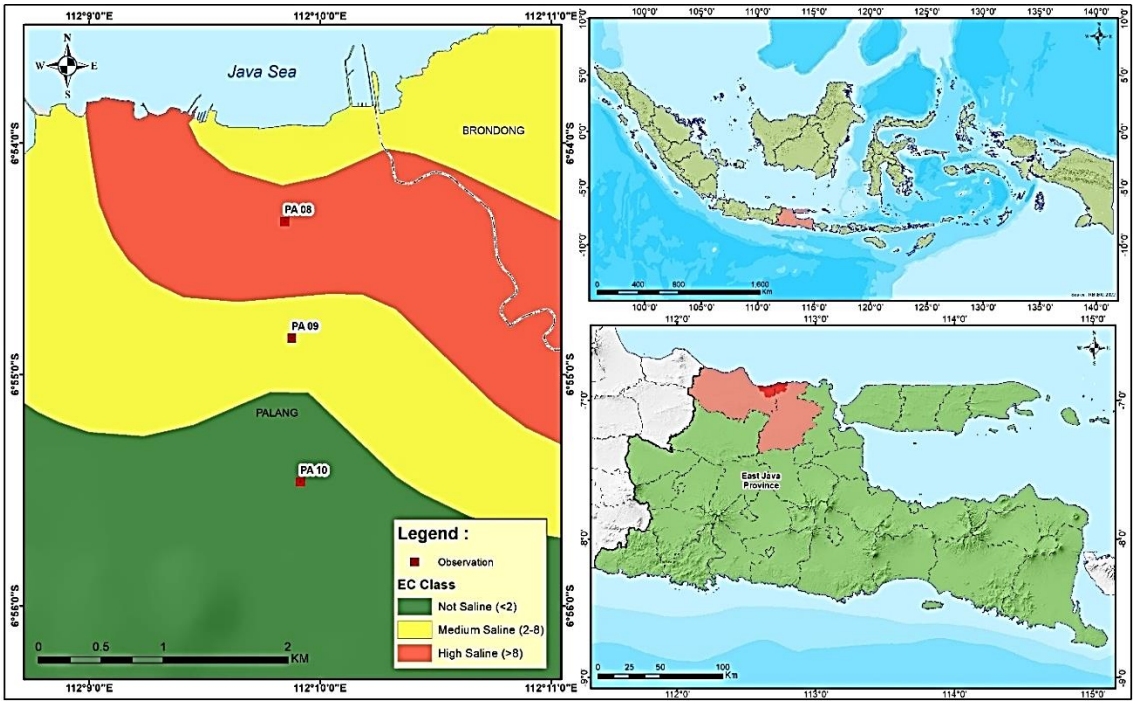

Fig. 1: Geographical location of the study area and sampling locations in Palang Subdistrict, Tuban Regency, East Java, Indonesia. (PA8, PA9, and PA10 represent the highest-, intermediate-, and lowest-EC sites in the present three-site comparison, respectively. The background EC strata shown in the original field map (<2, 2–8, and >8 dS/m) were used only for preliminary reconnaissance and are not treated as replicated salinity classes in the revised analysis)

which was decontaminated with water between successive sampling sites to prevent cross-contamination. The five subsamples were manually mixed and homogenized on a clean tray or clean plastic surface, yielding approximately 2.5 kilograms (kg) of bulk soil per site. A 100 g aliquot of each homogenized composite sample was placed in a clean resealable plastic ziplock bag for molecular analysis. The molecular aliquots were frozen for approximately 24 hours (h) in the freezer compartment of a two-door refrigerator before shipment. To maintain cold chain integrity during transit, specimens were transported in insulated, aluminum-foil-lined containers equipped with ice packs via priority overnight delivery, departing midday and arriving at the analytical facility on the subsequent afternoon. Due to the absence of continuous temperature logging during shipment, precise transit temperatures are not formally documented. Thus, each site contributed one composite biological sequencing sample; compositing improved within-site spatial coverage but did not create independent biological replication. Separate homogenized material from the same site composite was used for physicochemical analysis and was air-dried, gently crushed, and sieved through a 2 millimeters (mm) sieve before analysis (Carter and Gregorich, 2008; Sparks *et al.*, 1996).

Soil physicochemical analysis

Soil physicochemical characterization included EC, pH, organic carbon (C), exchangeable sodium (Na), potassium (K), calcium (Ca), and magnesium (Mg), cation exchange capacity (CEC), gravimetric moisture content, available and potential phosphorus (P), and particle-size distribution. EC was determined using a 1:5 soil-to-water suspension. A 10 g portion of air-dried soil passed through a 2 mm sieve was mixed with 50 milliliters (mL) of distilled water, mechanically shaken for 1 h, and measured with a conductivity meter. The procedure followed the approach reported previously (Eviati *et al.*, 2023). The soil chemical

properties and pH values detailed in Table 1 were derived from official analytical reports issued by the East Java soil laboratory reports. Soil pH was measured electrometrically at a 1:5 soil-to-water (H_2O) ratio. Soil organic carbon content was quantified using the Walkley and Black (1934) wet oxidation procedure coupled with spectrophotometric determination. Exchangeable K, Ca, Mg, and Na were extracted by percolation with 1 molar per liter (mol/L) ammonium acetate (NH_4OAc) at pH 7 and measured by atomic absorption spectrometry. CEC was determined by NH_4OAc percolation followed by 10 percent (%) sodium chloride (NaCl) displacement and titrimetry. Moisture content was determined gravimetrically by oven drying, available P by the Olsen method, potential P by 25% hydrochloric acid extraction, and texture by the hydrometer method. In accordance with laboratory advisories noting that cumulative extractable base cations may surpass measured CEC thresholds, individual cation and CEC values were retained as descriptive measurements but were not utilized to derive base saturation or exchangeable sodium percentage (ESP), prompting the exclusion of ESP from the refined analytical framework. Culturable bacterial abundance was determined by the total plate count (TPC) method on Nutrient Agar. Soil samples were stored frozen for approximately 2–3 days before analysis. A 1 g aliquot was taken while still partially frozen and mixed with 9 mL sterile 0.85% NaCl solution to obtain a 10−1 suspension. After vortex homogenization, tenfold serial dilutions were prepared to 10−6, with each tube vortexed before transfer. Aliquots of 1 mL from the 10−3, 10−4, and 10−5 dilutions were plated in duplicate by the pour-plate method with molten Nutrient Agar allowed to cool until warm. Plates were incubated at room temperature for 24 h. Bacterial enumeration was performed on replicate plates containing between 30 and 300 colonies per plate. The corresponding mean counts were adjusted using the reciprocal dilution factor to quantify culturable bacterial density in colony-forming units (CFU)/g soil (Pepper and Gerba, 2015).

Bacterial gene sequencing and taxonomic analysis

Deoxyribonucleic acid (DNA) extraction was performed by PT Aurora on the composite soil aliquots using the VAMNE Magnetic Stool/Soil DNA Extraction Kit (DMA5101, Vazyme Biotech Co., Ltd.) following the manufacturer's soil-DNA protocol. The manufacturer specifies 200 mg soil input for sample pretreatment with Lysis Buffer/ribonuclease A (RNase A), followed by mechanical disruption, inhibitor removal with the manufacturer-designated inhibitor-removal buffer, magnetic-bead binding and washing, and low-salt elution. The exact soil mass processed for each of the three extracts was not recorded in the documentation available to the authors and is therefore not stated as a sample-specific value. Furthermore, the available laboratory records lacked documentation regarding distinct absorbance-ratio acceptance thresholds at 260/280 nm and 260/230 nm, as well as the corresponding extraction-blank results. Downstream amplicon qualification, however, was documented by the sequencing provider using 0.8% agarose-gel examination and Qubit 2.0 fluorometry before pooling. Nearly full-length 16S rRNA genes were amplified with barcoded 27F (AGRGTTYGATYMTGGCTCAG) and 1492R (RGYTACCTTGTTACGACTT) primers. Polymerase chain reaction (PCR) was performed in 25 µL reactions containing 2× KAPA HiFi HotStart ReadyMix, 2.5 micromolar per litter (µmol/L) forward and reverse primers, and approximately 10 ng DNA template. Thermal cycling comprised 95 degrees Celsius (°C) for 3 minutes (min); 25 cycles of 95 °C for 30 s, 57 °C for 30 s, and 72 °C for 1 min; followed by 72 °C for 1 min. Qualified PCR products were combined in equal proportions and purified using AMPure PB beads. A 600 ng pooled amplicon was utilized to prepare a single-molecule real-time (SMRT) library employing the SMRTbell Prep Kit 3.0. Sequencing was conducted on a PacBio Sequel IIe using an SMRT 8M Cell with chemistry version 2, and secondary processing was carried out using the SMRT analysis pipeline v11.0.0. The resulting reads had median lengths of approximately 1,449–1,549 base pairs (bp). Full-

length PacBio sequencing and subsequent 16S analysis were conducted by Genomics (Taiwan) under project ID NT260119024. Primer sequences were removed before amplicon sequence variant (ASV) inference using Cutadapt v4.6 (Martin, 2011) with minimum length 1, overlap 3, error rate 0.1, reverse-complement search, and discard-untrimmed. Bioinformatic processing used nf-core/ampliseq v2.14.0 (Straub *et al.*, 2020). Read quality was evaluated with FastQC sequence quality-control software v0.12.1 (Andrews, 2010) and summarized with MultiQC quality-control reporting software v1.27 (Ewels *et al.*, 2016). Sequence-variant inference used divisive amplicon denoising algorithm 2 (DADA2) v1.30.0 (Callahan *et al.*, 2016), and downstream analysis used the quantitative insights into microbial ecology 2 (QIIME 2) framework v2024.10.1 (Bolyen *et al.*, 2019). In DADA2 filterAndTrim, minLen and maxLen were 1,000 and 1,600 bp, respectively. Reads passing filtering were denoised using the DADA2 error model, dereplicated, and screened for chimeras to generate ASVs. Given that the dataset comprised PacBio long-read amplicons rather than than paired-end short reads, read merging was omitted. Taxonomy assignment was performed in QIIME 2 using a primer-specific Naive Bayes classifier (Bokulich *et al.*, 2018), which was trained on the SILVA ribosomal ribonucleic acid gene database (SILVA) version 138.2 reference set clustered at 99% similarity (Quast *et al.*, 2012; Robeson *et al.*, 2021). The 99% value refers to the reference-sequence set used for classifier construction and is not a taxonomic assignment threshold or evidence of 99% species identity. ASVs with taxonomic strings containing mitochondria or chloroplast were removed before downstream analyses. ASVs, rather than traditional species-level taxonomic assignments, served as the primary units for all diversity analyses. Furthermore, parameters not explicitly documented in the sequencing report were neither reconstructed nor inferred from software defaults.

Diversity and community structure analysis

Alpha diversity was summarized at the ASV level using observed ASV richness, the Shannon index (Shannon, 1948), and the Gini-Simpson index (Simpson, 1949). The number of observed ASVs measures detected richness, the Shannon diversity index integrates both richness and relative abundance distribution, and the Gini-Simpson index summarizes evenness while allocating greater weight to dominant populations. Sequencing-depth adequacy was assessed from rarefaction curves generated from the post-taxonomic-filter ASV table. For beta diversity, Bray-Curtis dissimilarity was selected to describe abundance-based compositional differences without phylogenetic information, whereas Weighted UniFrac incorporated both relative abundance and phylogenetic branch lengths. Pairwise distance relationships were visualized using principal coordinate analysis (PCoA) (Gower, 1966). Given that individual sites were represented by single composite samples, downstream alpha- and beta-diversity measures were interpreted strictly in a descriptive capacity without the application of inferential statistical tests. For Weighted UniFrac, the QIIME 2 provenance of the verified weighted_unifrac distance artifact was inspected directly. Representative ASV sequences were aligned with multiple alignment using fast fourier transform (MAFFT) in q2-alignment v2024.10.0 using 20 threads with parttree disabled. The alignment was masked using a maximum gap frequency of 1.0 and minimum conservation of 0.4, after which a phylogenetic tree was constructed with FastTree in q2-phylogeny v2024.10.0 using 20 threads and midpoint-rooted. Weighted UniFrac distance matrices were generated using the rooted tree within the QIIME 2 beta-phylogenetic framework. Hierarchical clustering was excluded, as a dataset of three observations is insufficient for reliable group-level inference and adds no independent analytical value beyond the pairwise distance matrix. The Bray-Curtis metric was originally described by Bray and Curtis (1957).

Predicted ecological function analysis

Predicted ecological functions were generated with FAPROTAX 2025 from the processed 16S rRNA taxonomic table (Louca *et al.*, 2016). By mapping prokaryotic taxa to curated putative ecological functions, FAPROTAX provides heuristic functional predictions grounded in taxonomy rather than direct measurements. For quantitative comparison among the three samples, the abundance assigned to each functional category was divided by the post-taxonomic-filter read total for that sample (42,745 reads for PA8, 81,678 for PA9, and 34,447 for PA10) and expressed as a percentage. Because individual taxa may be mapped to multiple functional groups within FAPROTAX, these categories are not mutually exclusive, precluding cumulative relative abundances of exactly 100%. Coverage was calculated as the proportion of post-filter reads belonging to taxa assigned to at least one FAPROTAX group. Selected profiles are summarized in Table 5. Consequently, these functional predictions should not be construed as direct measurements of functional-gene abundance, transcriptional activity, enzymatic rates, cellular abundance, or in situ metabolic processes.

Analytical reliability and reproducibility

Reliability and reproducibility were addressed at multiple stages of the workflow. Amplicon products were evaluated by 0.8% agarose-gel examination and Qubit 2.0 fluorometry before pooling. Read quality was evaluated using FastQC (v0.12.1) and aggregated via MultiQC (v1.27). Absolute read counts were preserved throughout primer trimming, DADA2 filtering, denoising, chimera removal, and taxonomic filtering. ASVs were generated using the DADA2 error model rather than similarity-based operational taxonomic unit clustering, and taxonomy was assigned with a primer-specific Naive Bayes classifier trained from SILVA 138.2. Rarefaction output was used to assess sequencing-depth behavior, and the Weighted UniFrac tree-construction workflow and distance artifact were verified directly from QIIME 2 provenance. FAPROTAX execution parameters, including the software workflow version, sample-specific normalization denominator, and annotation coverage metrics, were fully documented. For auditability, the raw reads are archived in the National Center for Biotechnology Information (NCBI) Sequence Read Archive (SRA). Parameters not documented in the laboratory or bioinformatic records were left unassigned rather than inferred from software defaults. While this practice safeguards workflow traceability, it does not compensate for the inherent lack of biological replication within EC conditions.

RESULTS AND DISCUSSION

Soil physicochemical characteristics across the three sites

The three sites showed distinct physicochemical profiles rather than a uniform gradient across all measured soil properties (Table 1). PA8 had the highest EC (13.68 dS/m) and exchangeable Na (30.71 cmol(+)/kg), together with the lowest CEC (12.83 cmol(+)/kg). PA10 had the lowest EC (0.50 dS/m) but the highest organic C (1.45%), CEC (28.41 cmol(+)/kg), Olsen-available P (42 mg/kg), potential P (1,110 mg/kg), and TPC (8.5×10^4 CFU/g). PA9 represented the intermediate-EC site (3.74 dS/m) and showed comparatively low organic C and P availability. Under the 1:5 soil–water EC criteria of Eviati *et al.* (2023), PA8, PA9, and PA10 corresponded to very high, high, and very low EC classes, respectively. All soils were classified as clay, but clay content varied substantially among sites. ESP and base saturation were not calculated from the reported exchangeable-cation and CEC values. Overall, the sites differed in salinity, Na status, carbon and nutrient availability, cation-retention capacity, and soil physical properties.Such co-variation is ecologically important because soluble salts and Na enrichment can impose osmotic and ionic constraints, whereas organic C, pH, nutrient availability, and soil physicochemical properties can modify microbial resource availability and habitat conditions (Basak *et al.*, 2022; Dong *et al.*, 2022; Xie *et al.*, 2017). Furthermore, Agricultural

Table 1: Physicochemical characteristics and total plate counts of soil samples from Three coastal sites in Palang, Tuban, East Java

Parameter	Unit	PA8	PA9	PA10
Electrical conductivity	dS/m	13.68	3.74	0.50
pH (H_2O)	–	8.50	8.04	8.80
Organic C	%	1.01	0.62	1.45
Exchangeable Na	cmol(+)/kg	30.71	4.15	4.84
Exchangeable K	cmol(+)/kg	2.67	0.49	0.23
Exchangeable Ca	cmol(+)/kg	41.62	44.25	49.73
Exchangeable Mg	cmol(+)/kg	28.45	7.20	6.08
Cation exchange capacity	cmol(+)/kg	12.83	22.02	28.41
Gravimetric moisture content	%	7.86	6.61	7.74
Olsen-available P	Mg/kg	18	8	42
Potential P	Mg/kg	640	550	1,110
Clay fraction	%	42	75	78
Textural class	–	Clay	Clay	Clay
Total plate count	$\times 10^4$ CFU/g	0.7	2.4	8.5

Note: PA8, PA9, and PA10 represent the highest-, intermediate-, and lowest-EC sites, respectively, in this three-site comparison. Exchangeable cations and CEC are presented as reported by the analytical laboratory. Because the summed exchangeable base cations exceeded the measured CEC in some samples, these values were not used to derive ESP or base saturation. TPC represents culturable bacterial abundance under the applied culture conditions. Gravimetric moisture content represents laboratory-determined soil moisture rather than in-situ field moisture.

management practices can additionally drive variations in soil bacterial communities through mediated effects on edaphic conditions (Lee *et al.*, 2020). Therefore, subsequent bacterial community differences among PA8, PA9, and PA10 should be interpreted as site-specific responses to contrasting physicochemical environments rather than as effects of EC alone. TPC served solely as a measure of culturable bacterial density under the applied culture conditions, precluding its use as an estimate of total bacterial abundance (Janssen *et al.*, 2002).

Sequencing quality, sequence variant processing, and taxonomic assignment

Sequencing and read-processing metrics are summarized in Table 2. Cutadapt retained 99.3–99.6% of reads after primer trimming. DADA2 input counts were 58,005 for PA8, 109,492 for PA9, and 63,589 for PA10, yielding 42,816, 81,885, and 34,586 non-chimeric reads, respectively, after filtering, denoising, and chimera removal. PA10 consequently showed a lower overall DADA2 retention rate (54.4%) than PA8 (73.8%) and PA9 (74.8%). Although FastQC and MultiQC indicated elevated sequence-duplication levels (79.0–86.2%), these metrics were retained solely as quality-control indicators, given that sequence recurrence alone does not confirm technical PCR duplicates. Rarefaction curves were therefore used as an additional assessment of sequencing depth rather than as evidence that differences in read retention were fully eliminated. The high sequence retention observed following primer trimming indicates that primer removal incurred minimal sequence loss. In contrast, the substantial reduction during DADA2 processing reflects the cumulative impact of quality filtering, error correction, ASV inference, and chimera removal. These steps are integral to DADA2-based processing of full-length PacBio 16S rRNA amplicons and are intended to distinguish biological sequence variants from sequencing and PCR-derived errors (Callahan *et al.*, 2019). The reduced retention of PA10 necessitates cautious interpretation of comparative richness values, given that alpha-diversity metrics can be influenced by unequal effective sequencing depth and filtering stringency. Rarefaction provides a useful means of evaluating the influence of uneven sequencing effort, but it does not by itself demonstrate that richness estimates are free from depth-related effects (Schloss, 2024). Likewise, FastQC duplication metrics quantify repeated sequences and may indicate enrichment bias, including PCR over-amplification, but they are not sufficient on their own to identify the origin of duplicated reads. Consequently, differences in

Table 2: Sequencing quality and sequence variant processing summary

Parameter	PA8	PA9	PA10
Sequencing mode	PacBio Sequel IIe	PacBio Sequel IIe	PacBio Sequel IIe
Cutadapt total processed	58,427	109,973	63,981
Cutadapt passing filters	58,005	109,492	63,589
DADA2 input	58,005	109,492	63,589
DADA2 filtered	56,332	106,240	61,624
DADA2 denoised	43,485	82,776	34,820
DADA2 non-chimeric	42,816	81,885	34,586
Reads after taxonomic filtering	42,745	81,678	34,447
DADA2 non-chimeric retention (%)	73.8	74.8	54.4
FastQC sequence duplication (%)	84.2	86.2	79.0
Median read length (bp)	1,549	1,499	1,449
Mean Phred quality score	~40	~40	~40

sequencing depth and retention served strictly as methodological context for the descriptive analyses rather than as evidence of biological divergence among PA8, PA9, and PA10.

Alpha diversity of bacterial communities

Alpha-diversity profiles differed descriptively among the three sites (Table 3). PA9 showed the highest observed ASV richness (5,205) and Shannon diversity (11.39), followed by PA10 with 3,145 ASVs and a Shannon index of 11.03, whereas PA8 had the lowest values (2,052 ASVs; Shannon = 9.61). Gini-Simpson indices were consistently high, ranging from 0.9951 at PA8 to 0.9993 at PA10, indicating low dominance across the three communities. The Chao1 index was omitted from final evaluations since processed values matched observed ASV richness and lacked verifiable singleton or doubleton counts. Rarefaction curves were instead implemented to gauge sequencing-depth behavior. The lower richness and Shannon diversity at PA8 coincided with the highest EC and exchangeable Na, which is consistent with reports that elevated salinity can impose environmental filtering and reduce microbial diversity in salt-affected soils (Canfora *et al.*, 2014; Zhang *et al.*, 2019). However, bacterial diversity does not respond uniformly to salinity. Zhao *et al.* (2018) showed that pH can be as important as salinity in structuring bacterial communities, while Dong *et al.* (2022) reported strong compositional shifts without a corresponding reduction in bacterial richness. The higher richness at PA9 therefore should not be interpreted as evidence that intermediate EC maximized bacterial diversity. PA9 also had the greatest post-taxonomic-filter sequencing depth (81,678 reads), although PA10 contained fewer reads than PA8 yet retained greater observed richness, indicating that sequencing depth alone does not explain the observed ranking. Because uneven sequencing effort poses an ongoing technical challenge for alpha-diversity contrasts, rarefaction was employed as an additional safeguard to evaluate depth-dependent biases (Schloss, 2024). Because each site was represented by only one composite sequencing sample and soil properties and land use covaried with site identity, the alpha-diversity pattern is best interpreted as a site-specific outcome rather than a direct EC effect.

Table 3: Observed richness and alpha diversity indices of soil bacterial communities

Site	Observed ASVs	Shannon index	Gini-Simpson index
PA8	2,052	9.61	0.9951
PA9	5,205	11.39	0.9990
PA10	3,145	11.03	0.9993

Note: PA8 = highest-EC site; PA9 = intermediate-EC site; PA10 = lowest-EC site in the present three-site comparison.

Bacterial taxonomic composition across the three sites

Significant compositional divergence in bacterial communities was observed among the three sites (Fig. 2). PA8 showed the greatest relative representation of Bacillota (24.54%) and Bacillales (21.38%), with *Incertae_Sedis_14* (13.43%) and *Thalassobacillus* (11.46%) as the most represented genera. PA9 showed near-equal proportions of Bacillota (20.12%) and

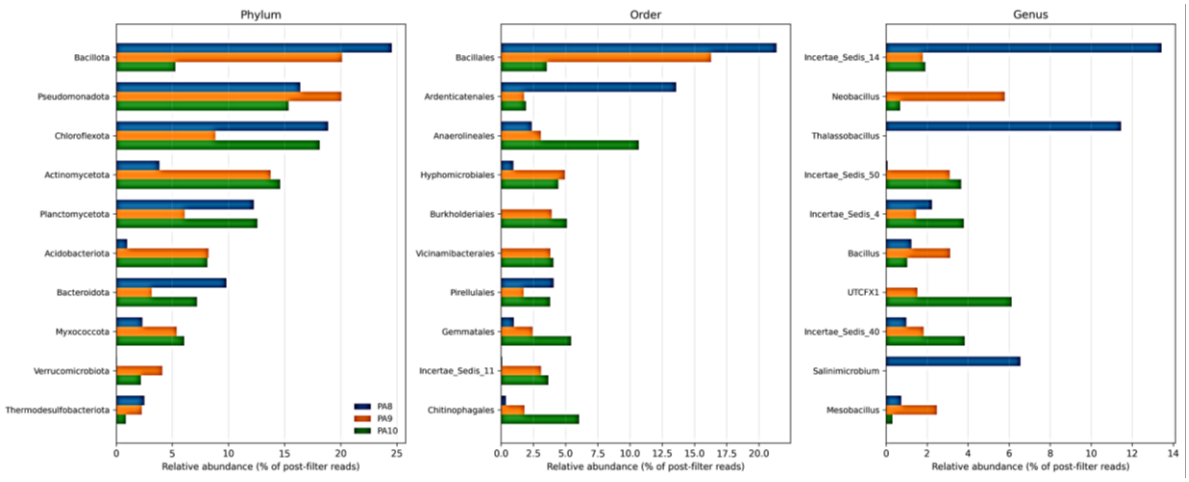

Fig. 2: Relative-abundance profiles of the ten bacterial taxa with the highest summed abundance across PA8, PA9, and PA10 at (a) phylum, (b) order, and (c) genus levels. Values represent percentages of all post-taxonomic-filter reads within each sample; taxa outside the displayed top ten are not shown. Each site is represented by one composite sequencing sample, and taxonomic differences are interpreted descriptively.

Pseudomonadota (20.07%), with Bacillales (16.30%) and *Neobacillus* (5.79%), whereas PA10 was characterized by Chloroflexota (18.14%), Anaerolineales (10.69%), and UTCFX1 (6.12%). These percentages were calculated relative to the total post-filtering read count per sample, thereby reflecting relative sequence proportions rather than absolute bacterial population size (Props *et al.*, 2017). The greater representation of Bacillota/Bacillales and *Thalassobacillus* at PA8 is ecologically compatible with previous evidence that saline conditions can restructure bacterial communities and favor lineages possessing greater salt tolerance (Dong *et al.*, 2022; Rath *et al.*, 2019). Consequently, observed profile differences cannot be isolated to EC owing to confounding variations in salinity, edaphic properties, and land management across PA8, PA9, and PA10. The detected taxa are therefore interpreted as site-associated community configurations rather than salinity-selected populations. Species-level annotations were excluded from the main ecological interpretation. Nearly full-length 16S rRNA sequencing provides substantially greater taxonomic resolution than partial-gene sequencing and, when combined with high-accuracy PacBio sequencing and appropriate denoising, can discriminate closely related sequence variants (Callahan *et al.*, 2019; Johnson *et al.*, 2019). Notwithstanding its advantages, full-length 16S profiling remains limited in achieving absolute species-level discrimination because sequence overlap occurs among distinct taxa, and multiple, divergent 16S gene variants can coexist within a single genome. Ecological interpretation was therefore restricted to phylum-, order-, and genus-level patterns.

Dominant bacterial taxa across the three sites

Table 4 highlights distinct taxonomic configurations among the three sites. PA8 was characterized by Bacillota (24.54%), Bacillales (21.38%), and *Incertae_Sedis_14* (13.43%); PA9 by near co-representation of Bacillota and Pseudomonadota (20.12% and 20.07%), Bacillales (16.30%), and *Neobacillus* (5.79%); whereas PA10 was characterized by Chloroflexota (18.14%), Anaerolineales (10.69%), and UTCFX1 (6.12%). The observed variations reveal localized reorganization of bacterial relative abundance across sites rather than a linear or continuous taxonomic transition in response to the EC gradient. Salinity can act as an environmental filter and alter bacterial community composition, but its effects commonly covary with pH, organic matter, and other edaphic conditions, making causal attribution difficult in field gradients (Dong *et al.*, 2022; Rath *et al.*, 2019). Furthermore, the

Table 4: Dominant bacterial taxa at phylum, order, and genus levels across the three sites

Taxonomic level	PA8 / highest EC	Relative abundance (%)	PA9 / intermediate EC	Relative abundance (%)	PA10 / lowest EC	Relative abundance (%)
Phylum	Bacillota	24.54	Bacillota / Pseudomonadota	20.12 / 20.07	Chloroflexota	18.14
Order	Bacillales	21.38	Bacillales	16.30	Anaerolineales	10.69
Genus	Incertae_Sedis_14	13.43	Neobacillus	5.79	UTCFX1	6.12

elevated relative abundance of *Thalassobacillus* at PA8 aligns with the known halophilic traits of this genus, which is frequently documented in saline soils and other hypersaline ecosystems (Tuesta-Popolizio *et al.*, 2021). Nevertheless, the present data do not demonstrate physiological salt tolerance or salinity-driven selection of the detected taxa because EC varied together with land use, organic C, exchangeable cations, CEC, and other site properties. PA9 and PA10 should therefore likewise be interpreted as distinct site-associated taxonomic assemblages rather than communities specifically selected by intermediate or low EC.

Heatmap patterns of dominant bacterial taxa

The genus-level heatmap revealed distinct site-associated abundance patterns (Fig. 3). PA8 was distinguished by the high relative representation of *Incertae_Sedis_14* (13.43%), *Thalassobacillus* (11.46%), *Salinimicrobium* (6.56%), and *Microbulbifer* (4.67%), whereas PA9 showed greater representation of *Neobacillus*, *Bacillus*, and *Mesobacillus*. PA10 displayed a contrasting profile dominated by UTCFX1 and several unresolved *Incertae_Sedis* groups. The prevalence of *Thalassobacillus* at PA8 is ecologically expected given the classification of this genus as a moderate-to-extreme environmental halophiles (Tuesta-Popolizio *et al.*, 2021). Collectively, prior studies on saline environments demonstrate that progressive salinization alters bacterial community composition through selective osmotic and ionic pressures, though both the scale and taxonomic composition of these responses are tightly governed by local environmental factors (Nan *et al.*, 2022; Rath *et al.*, 2019; Zhang *et al.*, 2024). The phylum-level heatmap reinforced this site differentiation (Fig. 4). PA8 was characterized by greater representation of Bacillota, whereas PA9 showed near co-representation of Bacillota and Pseudomonadota, and PA10 showed greater representation of Chloroflexota together with Actinomycetota and Planctomycetota. Chloroflexota comprises phylogenetically and metabolically diverse lineages occurring across terrestrial and aquatic environments; its higher representation at PA10 therefore cannot be assigned to a specific ecological function from 16S data alone (Wiegand *et al.*, 2023). The distinct clustering patterns are best understood as site-specific taxonomic assemblages rather than isolated responses to salinity, because EC shared strong collinearity with land-use practices, organic carbon, exchangeable cations, CEC, and broader environmental gradients. This caution is particularly important in field salinity studies, where salinity effects can be difficult to separate from co-varying edaphic factors (Dong *et al.*, 2022; Rath *et al.*, 2019).

Beta diversity and bacterial community structure

PCoA provided a descriptive visualization of differences among the three composite bacterial communities identified (Fig. 5). Non-phylogenetic compositional dissimilarity evaluated via Bray–Curtis ordination placed PA8, PA9, and PA10 at distinct coordinates, axes PCoA1 and PCoA2 accounted for 53.42% and 46.58% of the explained variation, respectively. Weighted UniFrac, which additionally incorporates phylogenetic branch lengths and relative abundance, showed the strongest separation of PA8, with distances of 0.4850 to PA9 and 0.5226 to PA10, compared with 0.3266 between PA9 and PA10. This concordance between abundance-based and phylogenetic outcomes reveals that the three sites variations involved shifts both in taxonomic relative abundance and in the structural distribution of

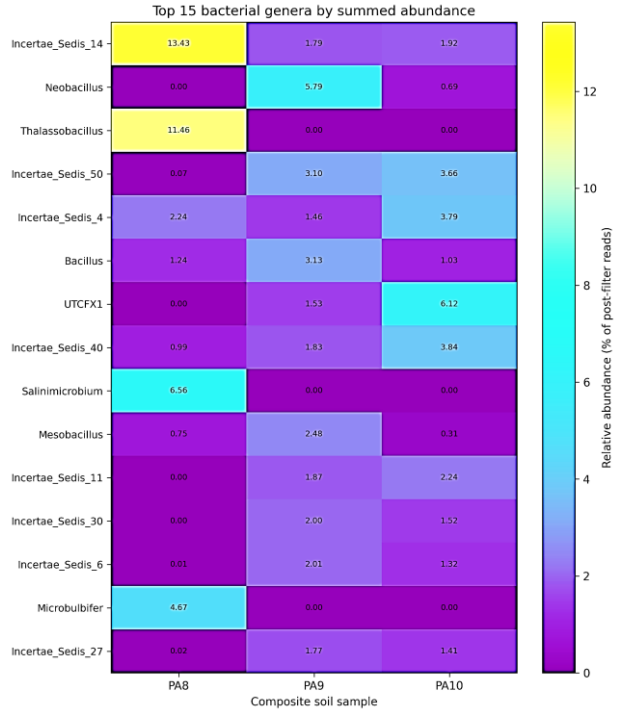

Fig. 3: Heatmap of the 15 bacterial genera with the highest summed abundance across PA8, PA9, and PA10. Cell values represent within-sample relative abundance based on all post-taxonomic-filter reads; no z-score standardization or clustering was applied

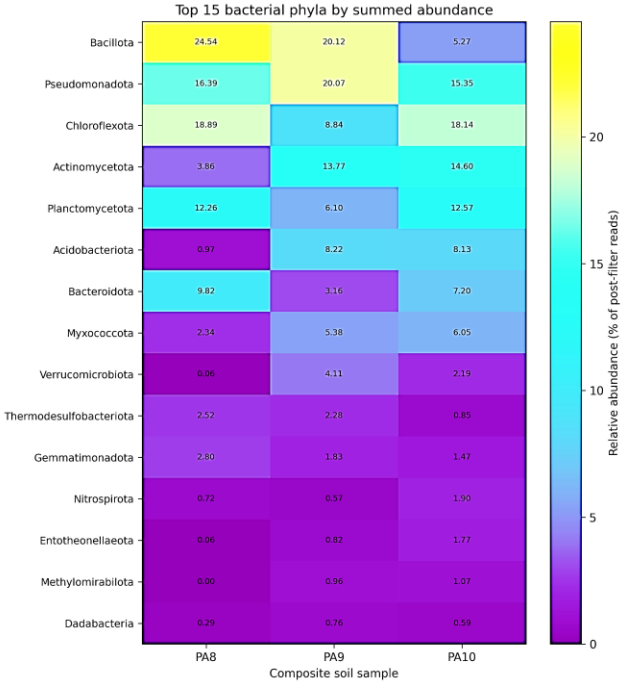

Fig. 4: Heatmap of the 15 bacterial phyla with the highest summed abundance across PA8, PA9, and PA10. Cell values represent within-sample relative abundance based on all post-taxonomic-filter reads; no z-score standardization or clustering was applied

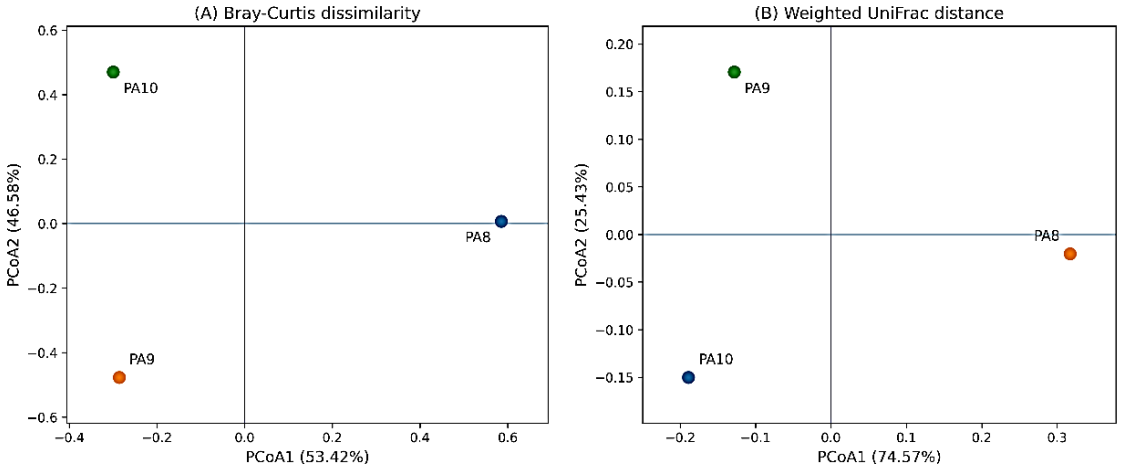

Fig. 5: Principal coordinate analysis (PCoA) of the three composite soil bacterial communities based on (A) Bray-Curtis dissimilarity and (B) Weighted UniFrac distance. Bray-Curtis PCoA1 and PCoA2 represent 53.42% and 46.58% of the displayed variation, whereas Weighted UniFrac PCoA1 and PCoA2 represent 74.57% and 25.43%, respectively. Each point represents one composite sequencing sample from PA8, PA9, or PA10. The ordinations are descriptive and do not represent replicated salinity treatments or inferential group comparisons

phylogenetically distinct lineages (Lozupone *et al.*, 2007; Lozupone and Knight, 2005). The greater phylogenetic dissimilarity of PA8 is consistent with its distinct taxonomic profile, including greater relative representation of Bacillota/Bacillales and several site-associated genera. Salinity serves as a key selective force influencing bacterial assemblage composition; however, the ubiquitous co-variance of field salinity gradients with auxiliary edaphic parameters limits the direct attribution of community shifts to salinity alone (Dong *et al.*, 2022; Rath *et al.*, 2019). In the present study, PA8 also differed in land use, exchangeable Na, CEC, and other measured and unmeasured environmental characteristics; its separation in ordination space is therefore interpreted as site-specific community differentiation rather than evidence of a salinity-driven treatment effect. Owing to the lack of replication (one composite sample per site), estimating within-condition variability was not feasible, thereby constraining the analytical design to descriptive comparisons in the absence of justifiable inferential testing (Anderson, 2001).

Predicted ecological functions of bacterial communities

FAPROTAX indicated distinct site-specific functional potentials related to carbon, nitrogen, and sulfur transformations (Table 5). Functional prediction indicated that Chemoheterotrophy constituted the primary metabolic pathway across the study sites (reaching 23.88% at PA10, 20.46% at PA8, and 16.97% at PA9), whereas proportional representation for aerobic chemoheterotrophy was maximized at PA9 and PA10. PA8 showed a particularly distinctive predicted profile, with substantially higher nitrate reduction (11.46%) and greater representation of aromatic-compound degradation, cellulolysis, xylanolysis, and chitinolysis relative to the alternative sites. Sulfate respiration was also more represented at PA8 and PA9 than at PA10. These contrasts are consistent with the different taxonomic compositions observed among the sites because FAPROTAX assigns ecological functions from taxonomic identities based on documented functions of cultured representatives rather than from direct measurements of functional genes or metabolic activity (Louca *et al.*, 2016; Sansupa *et al.*, 2021). The functional predictions should therefore be interpreted cautiously. Only 34.36%, 19.97%, and 26.07% of reads from PA8, PA9, and PA10, respectively, were assigned to at least one FAPROTAX category, indicating that substantial portions of the communities were outside the available functional annotations. Because predicted functional profiles derive directly from

Table 5: Selected FAPROTAX-predicted functional profiles expressed as percentage of post-taxonomic-filter reads

Predicted ecological function	PA8 (%)	PA9 (%)	PA10 (%)
Chemoheterotrophy	20.46	16.97	23.88
Aerobic chemoheterotrophy	3.98	8.41	7.86
Nitrate reduction	11.46	1.37	3.47
Aromatic compound degradation	5.22	1.70	0.62
Cellulolysis	4.68	0.29	0.19
Xylanolysis	4.67	0.03	0.00
Chitinolysis	4.67	0.01	0.00
Sulfate respiration	2.52	2.28	0.85
Fermentation	0.87	0.68	0.99
Methylotrophy	0.00	0.49	0.06
Methanotrophy	0.00	0.49	0.06
Ureolysis	0.00	0.31	0.39
Coverage: reads assigned to ≥1 FAPROTAX group	34.36	19.97	26.07

taxonomic assignments, they cannot substitute for direct measurements of gene abundance, metabolic expression, enzymatic kinetics, or in-situ biogeochemical turnover rates. This methodological constraint is supported by previous findings demonstrating that FAPROTAX generates valuable ecological hypotheses for soil bacterial communities yet may omit functions or taxa, and that predicted carbon-, nitrogen-, and sulfur-cycling assemblages do not invariably align with empirically quantified functional genes (Sansupa *et al.*, 2021; Yang *et al.*, 2022). Accordingly, the higher predicted nitrate reduction and organic-substrate degradation at PA8, and the contrasting carbon- and sulfur-related profiles at PA9 and PA10, are interpreted as site-associated functional hypotheses rather than evidence that EC or salinity altered biogeochemical process rates.

Ecological synthesis of site-specific patterns

Across the three sites, bacterial richness, Shannon diversity, taxonomic composition, phylogenetic dissimilarity, and predicted functional profiles did not form a simple monotonic sequence with EC. PA8, the highest-EC and highest-Na concentrations, exhibited the lowest observed ASV richness and Shannon diversity alongside a distinct taxonomic and Weighted UniFrac profile. In contrast, site PA9, with intermediate EC, displayed the highest observed richness and diversity, whereas site PA10, with the lowest EC, showed intermediate richness paired with a divergent phylum-, order-, and genus-level configuration. This non-monotonic pattern is ecologically plausible because salinity can exert strong environmental filtering on soil microbial communities, while its effects on richness, community composition, and assembly may vary among soil environments and interact with other edaphic factors (Dong *et al.*, 2022; Zhang *et al.*, 2019). In addition, broader edaphic analyses show that soil microbial assemblages are governed by multivariate interactions involving salinity, pH, and organic carbon, with the relative importance of individual drivers contingent upon depth and local environmental conditions (Xie *et al.*, 2017). Several mechanisms could therefore plausibly contribute to the contrasts observed among PA8, PA9, and PA10, including osmotic and ionic filtering, differences in carbon and nutrient availability, pH and cation balance, soil physicochemical conditions, and land-use or management history (Dong *et al.*, 2024; Lee *et al.*, 2020; Zhang *et al.*, 2019). In parallel, recent metagenomic findings highlight that microbial adaptation to salinity is mediated by clade-specific physiological constraints and metabolic interactions involving carbon assimilation, underscoring the ecological complexity and context-dependency of these community-level shifts (Dong *et al.*, 2024). However, these environmental properties varied simultaneously with site identity in the present study, and each EC condition was represented by only one composite sequencing sample. Consequently, the relative contribution of EC, Na-related chemistry, carbon

availability, pH, land use, or other unmeasured environmental factors cannot be separated or ranked from the present dataset. Consequently, these findings are interpreted as hypothesis-generating evidence of site-specific bacterial ecological organization under contrasting environmental conditions rather than as definitive proof of a direct salinity-driven functional response.

Study limitations

Attribution to salinity is limited by the observational design. PA8, PA9, and PA10 are three geographically distinct sites, and EC covaried with organic C, exchangeable Na, CEC, land use, texture, and other measured or unmeasured properties. For example, PA8 had EC of 13.68 dS/m, organic C of 1.01%, exchangeable Na of 30.71 cmol(+)/kg, and CEC of 12.83 cmol(+)/kg. PA9 had corresponding values of 3.74 dS/m, 0.62%, 4.15 cmol(+)/kg, and 22.02 cmol(+)/kg. PA10 had values of 0.50 dS/m, 1.45%, 4.84 cmol(+)/kg, and 28.41 cmol(+)/kg. The limited sample size of three site-level observations precludes the statistical partitioning or adjustment required to isolate an independent effect of salinity from co-varying environmental factors. The observed bacterial differences are therefore interpreted as site-specific associations rather than salinity effects. The composite-sampling design improves spatial coverage within each sampled site but does not provide biological replication. Each sequencing sample pooled soil from five field points within a site. The physical pooling and homogenization of component points precluded independent sequencing, thereby preventing the quantification or retention of fine-scale spatial heterogeneity within the final dataset. Ecological significance is therefore restricted to a descriptive snapshot of the pooled bacterial community at each site at the time of sampling. The observed contrasts are useful for identifying candidate taxa, diversity patterns, and community-distance profiles for future testing, but they do not establish a population-level response for an EC condition. Furthermore, the lack of independent biological replication prevents formal statistical evaluation of salinity-driven community responses. Within-condition variance, standard errors, confidence intervals, and a treatment-level error term cannot be estimated from one composite sequencing observation per EC condition. Accordingly, group-level inferential tests, analysis of variance, and regression of microbial metrics against EC were not used to infer a salinity effect. PCoA, alpha-diversity values, relative-abundance profiles, and FAPROTAX outputs are presented descriptively only. The findings cannot be generalized to high-, intermediate-, or low-EC soil classes beyond the sampled sites. Further methodological constraints stem from the incomplete documentation of historical management practices, including irrigation regimes, fertilization protocols, drainage infrastructure, and prior land-use history. Laboratory gravimetric moisture was measured and is reported in Table 1; however, in-situ field soil moisture and soil temperature were not recorded. Moreover, 16S rRNA amplicon sequencing provides compositional relative-abundance data rather than absolute population sizes. TPC represents only culturable bacteria under the applied culture conditions, species-level assignments remain uncertain for many taxa, and FAPROTAX outputs are predictions rather than direct functional measurements. Collectively, these methodological constraints constrain causal and regional extrapolation, positioning the present findings as a site-specific, hypothesis-generating baseline.

CONCLUSION

Distinct variations in bacterial communities across high-, moderate- and low-salinity conditions were found in the saline agricultural soils located at time of sampling. High-salinity soil yielded peak values for EC and sodium saturation coupled with depressed organic carbon, minimal richness and Shannon diversity, a singular

taxonomic configuration, and distinct spatial ordination patterns. These distinctive ecoevolutionary patterns suggests that salinity and sodium accumulation acted as potent ecological filters limiting community breadth, while favoring the establishment of high-salt-tolerating bacterial taxa. Bacterial diversity, however, did not exhibit a linear decline relative to salinity gradient. Moderate soil salinity corresponded with peak richness and Shannon diversity, coinciding with elevated organic carbon content and cation exchange capacity. This pattern aligns with eco-evolutionary theory, suggesting that organic carbon availability partially buffers estuarine bacteria against salt stress, whereas high-salinity soils may experience a shift in which key metabolic generalists are supplanted by specialized, stress-tolerant taxa. The distinction between the samples from low-salinity soil and the other groups due to their bacterial profile was less in proximity with, also based on tick richness estimated by pneumonic acid as well as culturable bacteria abundance, suggesting a differential response of the indicators of bacterium exposure to conditions in which they thrive during analysis. Taxonomic composition underwent marked structural shifts along the salinity gradient. Bacillota and Bacillales were the primary phyla in the high-salinity soil, accompanied by salt-associated genera (*Thalassobacillus, Salinimicrobium* and *Microbulbifer*). Conversely, low-salinity soil exhibited a higher relative abundance of Chloroflexota, Anaerolineales and several uncultured indigenous bacterial lineages. These changes illustrate that salinity affected bacterial diversity, as well as the identity and relative dominance of taxa at multiple taxonomic levels. Collectively, ordination frameworks demonstrated that spatial variation in bacterial assemblages reflected multivariate edaphic interactions rather than a direct, singular response to soil salinity gradients. The high-salinity condition was most closely related to EC, exchangeable sodium percentage and exchangeable sodium and had negative loadings relative to most bacterial diversity attributes in the ordination space. The bacterial assemblages documented under moderate and low salinity exhibited stronger associations with organic carbon resources, alleviated salt constraints, and ionic homeostasis. These relationships underpin a multivariate understanding of how bacterial communities respond to saline soil environments. Functional prediction revealed potential role of indigenous bacterial communities in chemoheterotrophic carbon utilization, sulfur transformation, nitrogen cycling, fermentation and complex organic compounds degradation. These functional assignments reflect estimated ecological potential rather than direct measurements of empirical gene expression, enzymatic activity, or biogeochemical process rates. According to this assessment, the response of bacteria to salinity is thus linear on a bacterial richness scale and driven by salt concentration, sodium enrichment, organic carbon content and the soil cation balance. Moreover, indigenous bacterial communities not only serve as bioindicators of saline-soil conditions, but also represent potential microbial resources for bio-remediation and soil recovery under elevated salinity. However, functional gene analysis and direct measurements of microbial activity are required to confirm these predicted ecological roles.

AUTHOR CONTRIBUTIONS

L. Fauziah designed and formulated this study, conducted field sampling, analyzed the data, interpreted the results, and prepared the draft manuscript. N. Aini supervised this study, provided methodological guidance, participated in data interpretation, and critically reviewed the manuscript. Y. Nuraini contributed by supervising this study, providing methodological guidance, participating in data interpretation, and critically reviewing the manuscript. Soemarno contributed

to data interpretation and critically reviewed the manuscript. N.D. Lestari contributed to data interpretation and critically reviewed the manuscript. Djajadi also contributed to data interpretation and critically reviewed the manuscript. All authors have read and approved the final version of this manuscript.

ACKNOWLEDGEMENT

The authors gratefully acknowledge financial support from the Professor Grant Program of Universitas Brawijaya for the 2025 fiscal year. The support was provided under contract number [08254.6/UN.10.F0401/B/KS/2025]. The authors also acknowledge the National Research and Innovation Agency of the Republic of Indonesia for institutional support during this research. Appreciation is extended to the laboratory staff and field assistants for their technical assistance with soil sampling, microbial isolation, and molecular analysis.

CONFLICT OF INTEREST

The authors declare that there is no conflict of interest regarding the publication of this manuscript. In addition, all relevant ethical requirements were observed by the authors. These include plagiarism, informed consent, misconduct, data fabrication and/or falsification, double publication and/or submission, and redundancy.

OPEN ACCESS

©2027 The author(s). This article is licensed under a Creative Commons Attribution 4.0 International License, which permits use, sharing, adaptation, distribution and reproduction in any medium or format, as long as you give appropriate credit to the original author(s) and the source, provide a link to the Creative Commons license, and indicate if changes were made. The images or other third-party material in this article are included in the article's Creative Commons license, unless indicated otherwise in a credit line to the material. If material is not included in the article's Creative Commons license and your intended use is not permitted by statutory regulation or exceeds the permitted use, you will need to obtain permission directly from the copyright holder. To view a copy of this license, visit: http://creativecommons.org/licenses/by/4.0/

PUBLISHER'S NOTE

GJESM Publisher remains neutral with regard to jurisdictional claims in published maps and institutional affiliations.

POSITIVE AI STATEMENT

During manuscript preparation, ChatGPT, an AI tool developed by OpenAI, was used for English-language editing and editorial assistance. This included grammatical correction, sentence restructuring, improved clarity and organization, and refinement of author-prepared scientific text. The tool was also used to improve the presentation of interpretations developed by the authors from the original data and analyses. ChatGPT was not used to generate, modify, fabricate, or replace experimental data, laboratory results, statistical outputs, or bioinformatic results. It was also not used to independently determine the study methodology or scientific conclusions. All AI-assisted suggestions were critically reviewed, verified against the original data and relevant literature, and revised by the authors. The authors retain full responsibility for the accuracy, integrity, and final content of this publication.

ABBREVIATIONS

%	Percent
°C	Degrees Celsius
16S rRNA	16S ribosomal ribonucleic acid
µmol/L	Micromolar per liter
AI	Artificial intelligence
ASV	Amplicon sequence variant
bp	Base pair
C	Carbon
Ca	Calcium

CEC	Cation exchange capacity
CFU	Colony-forming unit
cm	Centimeter
cmol(+)/kg	Centimoles of positive charge per kilogram of soil
DADA2	Divisive Amplicon Denoising Algorithm 2
DNA	Deoxyribonucleic acid
dS/m	Decisiemens per meter
E	East
EC	Electrical conductivity
ESP	Exchangeable sodium percentage
FAPROTAX	Functional Annotation of Prokaryotic Taxa
FastQC	FastQC sequence quality-control software
g	Gram
H_2O	Water
h	Hour
K	Potassium
kg	Kilogram
MAFFT	Multiple alignment using fast fourier transform
m	Meter
min	Minute
Mg	Magnesium
mL	Milliliter
mm	Millimeter
mol/L	Molar per liter
MultiQC	MultiQC quality-control reporting software
Na	Sodium
NaCl	Sodium chloride
NCBI	National Center for Biotechnology Information
nm	Nanometer
NH_4OAc	Ammonium acetate
P	Phosphorus
PA8	Highest-EC sampling site
PA9	Intermediate-EC sampling site
PA10	Lowest-EC sampling site
PCoA	Principal coordinate analysis
PCR	Polymerase chain reaction
pH	Potential of hydrogen
QIIME 2	Quantitative Insights Into Microbial Ecology 2
RNase A	Ribonuclease A
SILVA	SILVA ribosomal ribonucleic acid gene database
SMRT	Single-molecule real-time
S	South
SRA	Sequence Read Archive
TPC	Total plate count

REFERENCES

Anderson, M.J., (2001). A new method for non-parametric multivariate analysis of variance. Austral Ecol., 26(1): 32-46 **(15 pages)**.

Andrews, S., (2010). FastQC: a quality control tool for high throughput sequence data. Babraham Bioinformatics, Cambridge, UK.

Basak, N.; Rai, A.K.; Barman, A.; Mandal, S.; Sundha, P.; Bedwal, S.; Kumar, S.; Yadav, R.K.; Sharma, P.C., (2022). Salt affected soils: global perspectives. In: Salt affected soils: reclamation and management. Springer, Cham, Switzerland, 107-129 (**23 pages**).

Bokulich, N.A.; Kaehler, B.D.; Rideout, J.R.; Dillon, M.; Bolyen, E.; Knight, R.; Huttley, G.A.; Caporaso, J.G., (2018). Optimizing taxonomic classification of marker-gene amplicon sequences with QIIME 2's q2-feature-classifier plugin. Microbiome, 6(1): 90 (**17 pages**).

Bolyen, E.; Rideout, J.R.; Dillon, M.R.; Bokulich, N.A.; Abnet, C.C.; Al-Ghalith, G.A.; Alexander, H.; Alm, E.J.; Arumugam, M.; Asnicar, F.; Bai, Y.; Bisanz, J.E.; Bittinger, K.; Brejnrod, A.; Brislawn, C.J.; Brown, C.T.; Callahan, B.J.; Caraballo-Rodríguez, A.M.; Chase, J.; Cope, E.K.; Da Silva, R.; Diener, C.; Dorrestein, P.C.; Douglas, G.M.; Durall, D.M.; Duvallet, C.; Edwardson, C.F.; Ernst, M.; Estaki, M.; Fouquier, J.; Gauglitz, J.M.; Gibbons, S.M.; Gibson, D.L.; Gonzalez, A.; Gorlick, K.; Guo, J.; Hillmann, B.; Holmes, S.; Holste, H.; Huttenhower, C.; Huttley, G.A.; Janssen, S.; Jarmusch, A.K.; Jiang, L.; Kaehler, B.D.; Kang, K.B.; Keefe, C.R.; Keim, P.; Kelley, S.T.; Knights, D.; Koester, I.; Kosciolek, T.; Kreps, J.; Langille, M.G.I.; Lee, J.; Ley, R.; Liu, Y.X.; Loftfield, E.; Lozupone, C.; Maher, M.; Marotz, C.; Martin, B.D.; McDonald, D.; McIver, L.J.; Melnik, A.V.; Metcalf, J.L.; Morgan, S.C.; Morton, J.T.; Naimey, A.T.; Navas-Molina, J.A.; Nothias, L.F.; Orchanian, S.B.; Pearson, T.; Peoples, S.L.; Petras, D.; Preuss, M.L.; Pruesse, E.; Rasmussen, L.B.; Rivers, A.; Robeson, M.S.; Rosenthal, P.; Segata, N.; Shaffer, M.; Shiffer, A.; Sinha, R.; Song, S.J.; Spear, J.R.; Swafford, A.D.; Thompson, L.R.; Torres, P.J.; Trinh, P.; Tripathi, A.; Turnbaugh, P.J.; Ul-Hasan, S.; van der Hooft, J.J.J.; Vargas, F.; Vázquez-Baeza, Y.; Vogtmann, E.; von Hippel, M.; Walters, W.; Wan, Y.; Wang, M.; Warren, J.; Weber, K.C.; Williamson, C.H.D.; Willis, A.D.; Xu, Z.Z.; Zaneveld, J.R.; Zhang, Y.; Zhu, Q.; Knight, R.; Caporaso, J.G., (2019). Reproducible, interactive, scalable and extensible microbiome data science using QIIME 2. Nat. Biotechnol., 37(8): 852-857 **(6 pages)**.

Bray, J.R.; Curtis, J.T., (1957). An ordination of the upland forest communities of southern Wisconsin. Ecol. Monogr., 27(4): 325-349 (**25 pages**).

Callahan, B.J.; McMurdie, P.J.; Rosen, M.J.; Han, A.W.; Johnson, A.J.A.; Holmes, S.P., (2016). DADA2: high-resolution sample inference from Illumina amplicon data. Nat. Methods, 13(7): 581-583 (**3 pages**).

Callahan, B.J.; Wong, J.; Heiner, C.; Oh, S.; Theriot, C.M.; Gulati, A.S.; McGill, S.K.; Dougherty, M.K., (2019). High-throughput amplicon sequencing of the full-length 16S rRNA gene with single-nucleotide resolution. Nucleic Acids Res., 47(18): e103 (**12 pages**).

Canfora, L.; Bacci, G.; Pinzari, F.; Lo Papa, G.; Dazzi, C.; Benedetti, A., (2014). Salinity and bacterial diversity: to what extent does the concentration of salt affect the bacterial community in a saline soil? PLoS ONE, 9(9): e106662 (**15 pages**).

Carter, M.R.; Gregorich, E.G., (2008). Soil sampling and methods of analysis. 2nd ed. CRC Press, Boca Raton, USA (**1224 pages**).

Dong, Y.; Chen, R.; Graham, E.B.; Yu, B.; Bao, Y.; Li, X.; You, X.; Feng, Y., (2024). Eco-evolutionary strategies for relieving carbon limitation under salt stress differ across microbial clades. Nat. Commun., 15(1): 6013 (**12 pages**).

Dong, Y.; Zhang, J.; Chen, R.; Zhong, L.; Lin, X.; Feng, Y., (2022). Microbial community composition and activity in saline soils of coastal agro-ecosystems. Microorganisms, 10(4): 835 (**16 pages**).

Dreier, M.; Meola, M.; Berthoud, H.; Shani, N.; Wechsler, D.; Junier, P., (2022). High-throughput qPCR and 16S rRNA gene amplicon sequencing as complementary methods for the investigation of the cheese microbiota. BMC Microbiol., 22(1): 48 (**18 pages**).

Eviati; Sulaeman; Herawaty, L.; Anggria, L.; Usman; Tantika, H.E.; Prihatini, R.; Wuningrum, P., (2023). Petunjuk teknis edisi 3: Analisis kimia tanah, tanaman, air, dan pupuk. Kementerian Pertanian Republik Indonesia, Bogor, Indonesia (**271 pages**).

Ewels, P.; Magnusson, M.; Lundin, S.; Käller, M., (2016). MultiQC: summarize analysis results for multiple tools and samples in a single report. Bioinformatics, 32(19): 3047-3048 (**2 pages**).

Gower, J.C., (1966). Some distance properties of latent root and vector methods used in multivariate analysis. Biometrika, 53(3-4): 325-338 (**14 pages**).

Hailu, B.; Mehari, H., (2021). Impacts of soil salinity/sodicity on soil-water relations and plant growth in dry land areas: a review. J. Nat. Sci. Res., 12(3): 1-10 (**10 pages**).

Hindersah, R.; Pratiwi, E.; Fatma, Y.S.; Simarmata, T., (2023). Diversity and structure of bacterial communities in saline and non-saline rice fields in Cilacap Regency, Indonesia. Open Agric., 8(1): 20220225 (**11 pages**).

Janssen, P.H.; Yates, P.S.; Grinton, B.E.; Taylor, P.M.; Sait, M., (2002). Improved culturability of soil bacteria and isolation in pure culture of novel members of the divisions Acidobacteria, Actinobacteria, Proteobacteria, and Verrucomicrobia. Appl. Environ. Microbiol., 68(5): 2391-2396 (**6 pages**).

Johnson, J.S.; Spakowicz, D.J.; Hong, B.Y.; Petersen, L.M.; Demkowicz, P.; Chen, L.; Leopold, S.R.; Hanson, B.M.; Agresta, H.O.; Gerstein, M.; Sodergren, E.; Weinstock, G.M., (2019). Evaluation of 16S rRNA gene sequencing for species and strain-level microbiome analysis. Nat. Commun., 10(1): 5029 (**11 pages**).

Lee, S.A.; Kim, J.M.; Kim, Y.; Joa, J.H.; Kang, S.S.; Ahn, J.H.; Kim, M.; Song, J.; Weon, H.Y., (2020). Different types of agricultural land use drive distinct soil bacterial communities. Sci. Rep., 10(1): 17418 (**12 pages**).

Li, D.; Qiu, H.; Tian, G.; Zhao, Y.; Zhou, X.; He, S., (2023). Soil salinity is the main factor influencing the soil bacterial community assembly process under long-term drip irrigation in Xinjiang, China. Front. Microbiol., 14: 1291962 (**10 pages**).

Louca, S.; Parfrey, L.W.; Doebeli, M., (2016). Decoupling function and taxonomy in the global ocean microbiome. Science, 353(6305): 1272-1277 (**6 pages**).

Lozupone, C.; Knight, R., (2005). UniFrac: a new phylogenetic method for comparing microbial communities. Appl. Environ. Microbiol., 71(12): 8228-8235 (**8 pages**).

Lozupone, C.A.; Hamady, M.; Kelley, S.T.; Knight, R., (2007). Quantitative and qualitative beta diversity measures lead to different insights into factors that structure microbial communities. Appl. Environ. Microbiol., 73(5): 1576-1585 (**10 pages**).

Martin, M., (2011). Cutadapt removes adapter sequences from high-throughput sequencing reads. EMBnet.journal, 17(1): 10-12 **(3 pages)**.

Mucsi, M.; Borsodi, A.K.; Megyes, M.; Szili-Kovács, T., (2024). Response of the metabolic activity and taxonomic composition of bacterial communities to mosaically varying soil salinity and alkalinity. Sci. Rep., 14(1): 7460 (**15 pages**).

Nan, L.; Guo, Q.; Cao, S.; Zhan, Z., (2022). Diversity of bacterium communities in saline-alkali soil in arid regions of Northwest China. BMC Microbiol., 22(1): 11 (**12 pages**).

Pepper, I.L.; Gerba, C.P., (2015). Cultural methods. In: Pepper, I.L.; Gerba, C.P.; Gentry, T.J. (Eds.), Environmental microbiology. 3rd ed. Academic Press, San Diego, USA, 195-212 (**18 pages**).

Props, R.; Kerckhof, F.M.; Rubbens, P.; De Vrieze, J.; Hernandez Sanabria, E.; Waegeman, W.; Monsieurs, P.; Hammes, F.; Boon, N., (2017). Absolute quantification of microbial taxon abundances. ISME J., 11(2): 584-587 (**4 pages**).

Quast, C.; Pruesse, E.; Yilmaz, P.; Gerken, J.; Schweer, T.; Yarza, P.; Peplies, J.; Glöckner, F.O., (2012). The SILVA ribosomal RNA gene database project: improved data processing and web-based tools. Nucleic Acids Res., 41(D1): D590-D596 (**7 pages**).

Rath, K.M.; Fierer, N.; Murphy, D.V.; Rousk, J., (2019). Linking bacterial community composition to soil salinity along environmental gradients. ISME J., 13(3): 836-846 (**11 pages**).

Robeson II, M.S.; O'Rourke, D.R.; Kaehler, B.D.; Ziemski, M.; Dillon, M.R.; Foster, J.T.; Bokulich, N.A., (2021). RESCRIPt: reproducible sequence taxonomy reference database management. PLoS Comput. Biol., 17(11): e1009581 (**37 pages**).

Sansupa, C.; Wahdan, S.F.M.; Hossen, S.; Disayathanoowat, T.; Wubet, T.; Purahong, W., (2021). Can we use Functional Annotation of Prokaryotic Taxa (FAPROTAX) to assign the ecological functions of soil bacteria? Appl. Sci., 11(2): 688 (**17 pages**).

Schloss, P.D., (2024). Rarefaction is currently the best approach to control for uneven sequencing effort in amplicon sequence analyses. mSphere, 9(2): e00354-23 (**18 pages**).

Shannon, C.E., (1948). A mathematical theory of communication. Bell Syst. Tech. J., 27(3): 379-423 (**45 pages**).

Simpson, E.H., (1949). Measurement of diversity. Nature, 163(4148): 688 (**1 page**).

Sparks, D.L.; Page, A.L.; Helmke, P.A.; Loeppert, R.H.; Soltanpour, P.N.; Tabatabai, M.A.; Johnston, C.T.; Sumner, M.E., (1996). Methods of soil analysis. Part 3. Chemical methods. Soil Science Society of America, Madison, USA (**1390 pages**).

Straub, D.; Blackwell, N.; Langarica-Fuentes, A.; Peltzer, A.; Nahnsen, S.; Kleindienst, S., (2020). Interpretations of environmental microbial community studies are biased by the selected 16S rRNA (gene) amplicon sequencing pipeline. Front. Microbiol., 11: 550420 (**18 pages**).

Tarigan, R.; Lisnawita; Tantawi, A.R.; Hermanto, C., (2026). The impact of agroecological conditions on culturable bacterial and fungal diversity and soil chemical properties in chili pepper. Global J. Environ. Sci. Manage., 12(4): 2111-2132 **(22 pages).**

Tarolli, P.; Luo, J.; Park, E.; Barcaccia, G.; Masin, R., (2024). Soil salinization in agriculture: mitigation and adaptation strategies combining nature-based solutions and bioengineering. iScience, 27(2): 108830 (**8 pages**).

Tuesta-Popolizio, D.A.; Velázquez-Fernández, J.B.; Rodriguez-Campos, J.; Contreras-Ramos, S.M., (2021). Thalassobacillus, a genus of extreme to moderate environmental halophiles with biotechnological potential. World J. Microbiol. Biotechnol., 37(9): 147 (**13 pages**).

Utomo, B.; Dimyati, M.; Dewanti, R.; Trihatmoko, E.; Utami, P., (2026). Sustaining mangrove-based silvofishery to support coastal landscape resilience and explore ecotourism potential. Global J. Environ. Sci. Manage., 12(4): 1965-1988 **(24 pages).**

Walkley, A.; Black, I.A., (1934). An examination of the Degtjareff method for determining soil organic matter and a proposed modification of the chromic acid titration method. Soil Sci., 37(1): 29-38 (**10 pages**).

Wiegand, S.; Sobol, M.; Schnepp-Pesch, L.K.; Yan, G.; Iqbal, S.; Vollmers, J.; Müller, J.A.; Kaster, A.K., (2023). Taxonomic re-classification and expansion of the phylum Chloroflexota based on over 5000 genomes and metagenome-assembled genomes. Microorganisms, 11(10): 2612 (**19 pages**).

Xie, K.; Deng, Y.; Zhang, S.; Zhang, W.; Liu, J.; Xie, Y.; Zhang, X.; Huang, H., (2017). Prokaryotic community distribution along an ecological gradient of salinity in surface and subsurface saline soils. Sci. Rep., 7(1): 13332 (**10 pages**).

Yang, Z.; Peng, C.; Cao, H.; Song, J.; Gong, B.; Li, L.; Wang, L.; He, Y.; Liang, M.; Lin, J.; Lu, L., (2022). Microbial functional assemblages predicted by the FAPROTAX analysis are impacted by physicochemical properties, but C, N and S cycling genes are not in mangrove soil in the Beibu Gulf, China. Ecol. Indic., 139: 108887 (**15 pages**).

Yuliana, E.; Winata, A.; Setijorini, L.E.; Yani, D.E.; Fathani, M.H.; Djatmiko, W.A., (2026). Biodiversity-oriented criteria for measuring the effectiveness of mangrove ecosystem rehabilitation success. Global J. Environ. Sci. Manage., 12(4): 1619-1638 **(20 pages).**

Zhang, G.; Bai, J.; Zhai, Y.; Jia, J.; Zhao, Q.; Wang, W.; Hu, X., (2024). Microbial diversity and functions in saline soils: a review from a biogeochemical perspective. J. Adv. Res., 59: 129-140 (**12 pages**).

Zhang, K.; Shi, Y.; Cui, X.; Yue, P.; Li, K.; Liu, X.; Tripathi, B.M.; Chu, H., (2019). Salinity is a key determinant for soil microbial communities in a desert ecosystem. mSystems, 4(1): e00225-18 (**9 pages**).

Zhao, S.; Liu, J.J.; Banerjee, S.; Zhou, N.; Zhao, Z.Y.; Zhang, K.; Tian, C.Y., (2018). Soil pH is equally important as salinity in shaping bacterial communities in saline soils under halophytic vegetation. Sci. Rep., 8(1): 4550 (**11 pages**).

AUTHOR (S) BIOSKETCHES

Fauziah, L., Ph.D. Candidate, Postgraduate Program, Faculty of Agriculture, Brawijaya University, Jl. Veteran No. 10–11, Malang 65145, Indonesia; Researcher, Research Center for Estate Crops, Research Organization for Agriculture and Food, National Research and Innovation Agency of the Republic of Indonesia, Jl. Raya Jakarta–Bogor Km 46, Cibinong, Bogor 16911, Indonesia.
- Email: *lili025@brin.go.id*
- ORCID: 0000-0002-7515-574X
- Web of Science ResearcherID: QWC-1004-2026
- Scopus Author ID: 58157153600
- Homepage: https://simpeg.brin.go.id/admin/kepegawaian/pegawai/profilen

Nuraini, Y., Professor, Department of Soil Science, Faculty of Agriculture, Brawijaya University, Jl. Veteran No. 10–11, Malang 65145, Indonesia.
- Email: *ynuraini@ub.ac.id*
- ORCID: 0009-0002-3056-1135
- Web of Science ResearcherID: JLL-1344-2023
- Scopus Author ID: 56271859000
- Homepage: https://fbipk.ub.ac.id/profil-dosen/

Soemarno, Professor, Department of Soil Science, Faculty of Agriculture, Brawijaya University, Jl. Veteran No. 10–11, Malang 65145, Indonesia.
- Email: *smno@ub.ac.id*
- ORCID: 0000-0002-7058-6495
- Web of Science ResearcherID: JLL-7442-2023
- Scopus Author ID: 55876886500
- Homepage: https://fbipk.ub.ac.id/profil-dosen/

Lestari, N.D., Lecturer and Researcher, Department of Soil Science, Faculty of Agriculture, Brawijaya University, Jl. Veteran No. 10–11, Malang 65145, Indonesia.
- Email: *nd.lestari@ub.ac.id*
- ORCID: 0000-0002-0496-2819
- Web of Science ResearcherID: NA
- Scopus Author ID: 57205465015
- Homepage: https://fbipk.ub.ac.id/profil-dosen/

Djajadi, Professor and Researcher, Research Center for Estate Crops, Research Organization for Agriculture and Food, National Research and Innovation Agency of the Republic of Indonesia, Jl. Raya Jakarta–Bogor Km 46, Cibinong, Bogor 16911, Indonesia.
- Email: *djaj001@brin.go.id*
- ORCID: 0000-0003-0931-4519
- Web of Science ResearcherID: QWC-1160-2026
- Scopus Author ID: 55204846200
- Homepage: https://simpeg.brin.go.id/admin/kepegawaian/pegawai/profilen

Aini, N., Professor, Department of Agronomy, Faculty of Agriculture, Brawijaya University, Jl. Veteran No. 10–11, Malang 65145, Indonesia.
- Email: *nra-fp@ub.ac.id*
- ORCID: 0000-0002-7480-8243
- Web of Science ResearcherID: GPK-1954-2022
- Scopus Author ID: 57219657937
- Homepage: https://fbipk.ub.ac.id/profil-dosen/

HOW TO CITE THIS ARTICLE:
Fauziah, L.; Nuraini, Y.; Soemarno; Lestari, N.D.; Djajadi; Aini, N., (2027). Ecological diversity in soil properties and bacterial communities in tropical coastal areas with contrasting electrical conductivity. Global J. Environ. Sci. Manage., 13(1): 231-250.

DOI: 10.22034/gjesm.2027.01.11
URL: https://www.gjesm.net/article_735607.html